Pumping Liquid Crystals

Zhong Zou and Noel Clark
Department of Physics and Optoelectronic Computing Systems Center, University of Colorado, Boulder, Colorado 80309
(Received 30 November 1994)

We observe mass pumping of a ferroelectric smectic-C liquid crystal induced by an applied ac voltage. The flow is unidirectional, reflecting the chirality of the system. An elastohydrodynamic model of the smectic-C phase is used to explain the observations.

PACS numbers: 61.30.Gd

Liquid crystals combine the flow properties of liquids with the orientational order of crystals. The coupling of these two properties generates a rich elastic-hydrodynamic behavior and a variety of novel flow phenomena unique to liquid crystals [1]. In this Letter we report a remarkable electromechanical pumping effect in which the application of an ac voltage to a ferroelectric liquid crystal produces a chiral unidirectional pumping of the fluid in a direction normal to the applied ac field.

This effect is related to the orientation-flow coupling found in nematics that is responsible for "backflow" effects wherein driven molecular reorientation generates flow, which then in turn alters the reorientation [2,3]. Recently, Zou, Clark, and Carlsson have shown by computer simulation that a similar back switching would also appear in surface stabilized ferroelectric liquid crystals (SSFLC's) [4]. They have demonstrated the necessity of including the coupling of flow to molecular reorientation, first observed by Brochard, Pieranski, and Guyon [5], for a proper description of FLC dynamics, by numerically solving elastohydrodynamic equations derived [6,7] from Leslie, Stewart, and Nakagawa's (LSN) continuum theory of Sm-C liquid crystals [8] applied to FLC's. Experimentally, Jakli and Saupe [9] have demonstrated that, through electromechanical measurements, the reorientation of molecules can produce mechanical vibration of the bounding plates in cells, suggesting mass flow to be the origin of such mechanical motion [9]. Here we provide the first experimental evidence that mass flow (pumping) may be generated by liquid crystal molecular reorientation. Our numerical simulations are qualitatively comparable with the experimental results.

The FLC cell geometry used in the experiment is depicted in Fig. 1(a). The FLC is sandwiched between two glass substrates coated with indium tin oxide (ITO) transparent conducting film. The ITO of the bottom substrate (normal to $\hat{x}$) is divided into four rectangular pixel elements having a 20 mm length along $\hat{y}$ and a 3 mm width along $\hat{z}$. The top substrate, which is about 10 mm wide along $\hat{y}$, is uniformly coated with ITO. Nylon is coated over the ITO and rubbed parallel to $\hat{z}$ to align the liquid crystal director along $\hat{z}$, so that the layers align parallel to $\hat{y}$ in the smectic-A phase. Spacers are used to separate the two substrates to form the gap of thickness d containing the FLC. The ends of the cell along $\hat{z}$ (e.g., the two edges parallel to $\hat{y}$) are sealed so that there is no relative motion of the two substrates.

In the smectic-C phase the director $\vec{n}$ is confined to the tilt cone of cone angle θ. The $\vec{c}$ director is defined as the unit vector along the projection of $\vec{n}$ onto the smectic planes. The azimuthal angle ϕ is defined as the angle between the ferroelectric polarization $\vec{P}_s = P_s(\hat{z} \times \hat{c})$ and $\hat{x}$ taking ϕ positive for a right-hand rotation around the negative $\hat{z}$ axis. The electrical torque $(\vec{P}_x \times \vec{E})$ makes the $\vec{c}$ director rotate (in ϕ), and the reorientation of the $\vec{c}$ director drives the flow along $\hat{y}$. Flow along $\hat{z}$ requires permeation and flow along $\hat{x}$ is prohibited by the bounding plates. Both can be ignored. In order to observe the flow, the sides of the cell where the layers terminate are *open* and a second fluid is placed outside the cell [10]. This enables the FLC material (Merck ZLI3654) to transport along $\hat{y}$ and to move out of the cell with minimal interference of surface tension if the appropriate stress appears. A variety of second fluids were tested, including silicon oil, paraffin oil, glycerol, and water. The best results were obtained using a nematic LC (Roche RO-TN-132) as the second fluid. This is because this nematic is only slightly miscible with ZLI3654, has comparable viscosity retarding the diffusive mixing of the phases, is insulating, and forms a very low surface tension interface with the FLC. The cell is viewed in transmission between crossed polarizers and the image is relayed to a video camera.

We present data from two experimental runs in Fig. 1(b). Photos (i), (ii), and (iii) of Fig. 1(b) show a sequence of images of a $d = 5$ μm cell with alternate pixels held in opposite polarization states by a ± 1.7 V dc bias, and an 80 V peak-to-peak square wave voltage of frequency $f = 10$ kHz applied. The polarizer and the analyzer are arranged so that pixels 1 and 3 have higher transmission. The 10 kHz frequency is sufficiently high, $f\tau = 1.6$, where τ is the FLC electro-optic orientation response time, that the $\vec{c}$ director oscillates only about its dc stabilized state. Photos (i)–(iii) are the images at $t = 0$, 10, and 24 min, respectively. In Fig. 1(b), the black areas are the nematic LC's being drawn from outside the cell, as the FLC has been pumped by the voltage out to the other side. The area is black because the nematic molecules are aligned homeotropically in the

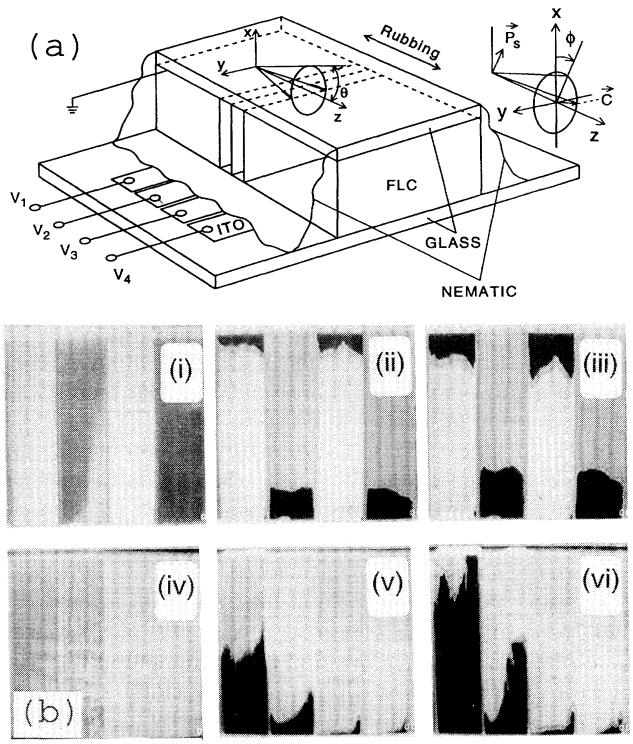

FIG. 1. (a) The SSFLC cell used in the pumping experiment. The cell is unsealed where the smectic layers intersect the cell edge. A second fluid, in this case a nematic, covers the unsealed edges so that if the FLC exits the cell the resulting void can be filled with minimal energy interfacial energy. The ITO electrode in the bottom plate is divided into four pixels. (b) Photo images of SSFLC cells under crossed polarizers show unidirectional pumping. The black areas are the nematic LC drawn into the cell. Photos (i)–(iii) are for a $d = 5$ μm cell with a 10 kHz, 80 V peak-to-peak square wave applied voltage, applied for $t = 0$, 10, and 24 min, respectively. Pixels (2,4) and (1,3) are held in opposite polarization states by a ± 1.7 V dc bias, respectively. Flow goes in one direction for the $(\vec{P}_s)_x > 0$ (white) state, and in the other direction for the $(\vec{P}_s)_x < 0$ (dark) state. Photos (iv)–(vi) (at $t = 0$, 11, and 21 min, respectively) show the voltage dependence of pumping for a $d = 10$ μm cell, pixels 1 to 4 are having 160, 120, 80, and 40 V peak-to-peak square wave voltage applied, respectively. The dc offset is -2 V. The pumping is faster as the voltage increases.

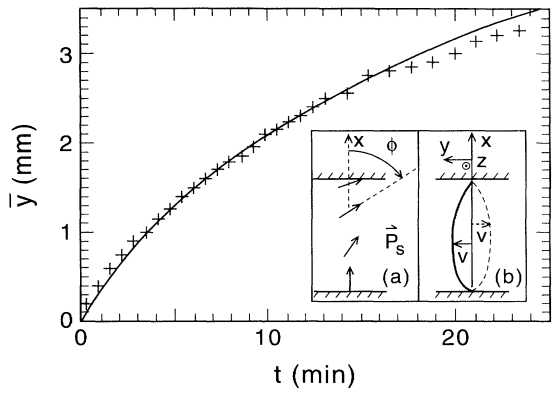

FIG. 2. Displacement of the FLC-nematic interface vs time. The + is the experimental data for the 5 μm cell in Fig. 1(b), and the solid curve is from the calculation. Inset (a) shows the configuration of $\vec{P}_s(x)$ when $V = 0$ used in the calculations ($\phi_s = 80°$). Inset (b) shows the typical flow velocity response to the positive part of applied square wave (the dashed curve) and to the negative part of applied square wave (the solid curve). This $\phi(x)$ lacks symmetry about the cell center and the resulting velocity lacks inversion symmetry about the cell center. Since the response $\delta\phi(x)$ is not symmetric with respect to the sign of E, there will be a net flow in response to the applied square wave.

ac electric field. Thus we see a net flow in one direction in the white state, and in the other direction in the dark state, reflecting the chiral asymmetry of the system. With bistable cells, we see the same effect under high frequency square wave electric field without applied dc. The displacement $\bar{y}$ of the FLC along $\hat{y}$ in pixel 2 vs time t is plotted in Fig. 2 as the + symbols. The net flow velocity of FLC will be the slope of the displacement curve. Figure 2 shows that the flow has the highest velocity at the beginning, then gradually slows down. The FLC-nematic interfaces initially move as straight lines parallel to $\hat{z}$ but tend to become irregular as the experiment proceeds, as Fig. 1(b) shows. The origin of the irregularity is not clear at this time but indicates that the flow is sensitive to FLC structural features, such as layering and surface anchoring defects. We have carried out experiments in cells with different FLC thickness d and also in wedged cells [11]. Generally our observations indicate that with same field amplitude and frequency the thicker cells have larger flow velocities than the thinner ones. The flow velocity also depends on the shape of the applied electric field wave form, the frequency, and the amplitude. Photos (iv)–(vi) of Fig. 1(b) (corresponding to $t = 0$, 11, and 21 min, respectively) show an example of the field dependence of the flow. Here $d = 10$ μm, and the dc offset is -2.0 V. The peak-to-peak voltage and the frequency are (160 V, 8 kHz), (120 V, 6 kHz), (80 V, 4 kHz), and (40 V, 2 kHz), for pixels 1, 2, 3, and 4, respectively. These are frequency-voltage combinations for which $f\tau$ is approximately constant and $f\tau \approx 1.3$. One can see immediately that the larger amplitude of the applied voltage generates faster flow.

The same experiments have been carried out for cells with rubbing direction of the alignment layer along $\hat{y}$, and the smectic-C layers along $\hat{z}$ in Fig. 1. No net flow has been observed in these experiments after applying ac field for about one day. This indicates that the flow is confined to be parallel to the smectic layer and that permeative flow is much smaller than the flow along the layers.

Why should there be a net flow under an ac electric field? A rotating $\vec{c}$ director applies a local torque to the LC behaving as a local "paddlewheel" to generate flow. The spatial structure of $\phi(x,t)$ determines the velocity $v_y(x,t)$. A net flow implies generally that $v_y(x,t)$ lacks

both inversion symmetry in x about the cell center and inversion symmetry in t about the times of transition of the square wave. Generally, these conditions will be present if $\phi(x)$ for $E = 0$ is neither symmetric nor inversion symmetric in x about the cell center [11]. The simplest $\hat{c}$-$\vec{P}_s$ distribution that will give net flow is shown in inset (a) in Fig. 2. Applied voltage induces different orientation change in the top and bottom halves of the cell. Furthermore, it is easy to see from the inset that the time varying orientation change $\delta\phi(E,t)$ is not antisymmetric in E around $E = 0$, i.e., $\delta\phi(t)_{E>0} \neq -\delta\phi(t)_{E<0}$. The result is that the velocity integral over x and the negative half cycle in t does not cancel the integral over x and the positive half cycle in t and there is a net flow. Inset (b) in Fig. 2 shows a typical velocity response to the positive part of the applied square wave (the dashed curve) and to the negative part of the square wave (the solid curve).

In order to calculate the molecular reorientation induced mass flow, we set up the applicable flow coupled switching equations [6,8] for SSFLC's. In doing so, we take the fluid as incompressible, neglect the permeation, and assume both flow velocity $\vec{v} = \vec{v}(x,t)$ and azimuthal orientation $\phi = \phi(x,t)$ are x and t dependent only. Then $\vec{v}(x,t) = v_y(x,t)\hat{y}$, with both $v_x(x,t)$ and $v_z(x,t)$ being zero, and we obtain the following equations for the balance of linear moments in the FLC and nematic regions respectively:

$$-\frac{\partial p(x,y,t)}{\partial y} + \frac{\partial}{\partial x}\left(F(\phi)\frac{\partial v_y(x,t)}{\partial x} + L(\phi)\frac{\partial\phi(x,t)}{\partial t}\right) = 0, \quad (1)$$

$$-\frac{\partial p^n(x,y,t)}{\partial y} + \mu^n\frac{\partial^2 v_y^n(x,t)}{\partial x^2} = 0. \quad (2)$$

The inertial terms are neglected [3,6]. The pressures are p and p^n, velocities v_y and v_y^n in the FLC and nematic region, respectively, and μ^n is the nematic viscosity. The $F(\phi)$ and $L(\phi)$ [4,6] are FLC viscosity parameters, and are both ϕ dependent. $F(\phi)\partial v_y/\partial x$ is the stress generated by shear flow, while $L(\phi)\dot{\phi}$ is the stress due to molecular reorientation. In this problem, we consider the flow to be uniform laminar [Reynolds number in SI units $R = (\rho/n)vd \approx (1000/0.1)10^{-3}10^{-5} < 1$] except near the FLC-nematic interface. The interfacial region size will be comparable to the cell thickness, which is about 10^{-3} of the cell length in the y direction. Thus it is reasonable to assume that $v_y(x,t)$ and $\phi(x,t)$ depend only on x. Therefore, from Eq. (1), $\partial p/\partial y$ and $\partial p^n/\partial y$ are y independent, and the pressures p and p^n vary linearly with y. This pressure gradient is the driving force for the nematic liquid crystal to move into the cell. The open cell boundary conditions are such that at the two edges along y are $p = p^n = p_0$, where p_0 is the atmospheric pressure, and at the nematic and FLC interface $p = p^n$. Because of the flow and incompressibility, the average of the flow velocities over the cell thickness along x should at all times be equal, e.g., $\bar{v}(t) = \bar{v}^n(t)$. With nonslip conditions at the substrates, one gets

$$\frac{\partial p}{\partial y} = \frac{12\bar{y}\mu^n}{(1-\bar{y})d^2}\bar{v}, \quad (3)$$

where $\bar{v} = d\bar{y}/dt$ and $\bar{y}$ is the net displacement of FLC material which is the displacement of the FLC-nematic interface. This equation accounts for the increased drag and reduced pumping with increasing $\bar{y}$ as the FLC leaves and the nematic enters the cell.

The calculation of $\bar{v}$ vs $\partial p/\partial y$ depends on the details of $\phi(x)$ and requires solution of the equation coupling ϕ and $\vec{v}$ in the FLC [4]. By combining Eq. (1) with the torque equation $\Gamma = K\partial^2\phi/\partial x^2 - P_sE\sin\phi = L(\phi)\partial v/\partial x + \eta\partial\phi/\partial t$, where η is the rotational viscosity of the FLC, K is the effective smectic-C Frank elastic constant, and Γ is the elastic and polarization torque, one obtains the complete set of equations describing the pumping effect. This set of equations requires numerical solution and was solved using procedures to be published elsewhere [11]. Here we present one such solution under an ac square wave field (with $f = 1.6/\tau$ and peak-to-peak voltage 80 V for a $d = 5$ μm thick cell), using the viscosities and polarizations given in Ref. [4], except $K = 12.68 \times 10^{-8}$ N/m^2 and $\theta = 25°$. The $\phi(x)$ at the $E = 0$ state for this calculation is shown in the inset in Fig. 2, the simplest $\phi(x)$ that is of low enough symmetry to give net flow. This $\phi(x)$ matches the symmetry of the commonly used half sprayed states found in chevron SSFLC cells [12]. The coupled equations are solved, and the resulting ϕ and v_y profiles are plotted in Figs. 3(a) and 3(b), respectively. Figure 3(c) shows the applied voltage and the corresponding flow velocity at the center of the cell, also indicated by the heavy curve in fig. 3(b). When the square wave voltage is applied, the LC molecules will oscillate around their equilibrium states driving an oscillatory velocity. The time axis is given in the units of the characteristic switching time $\tau = \eta/P_sE$, and the time interval plotted is two periods at $t \approx 3998\tau$ units, roughly 6400 cycles after the start of the square wave application, at which time the steady-state oscillation has been reached. The net displacement $\bar{y}$ is defined as $\bar{y}(t) = (1/d)\int_0^d\int_0^t v_y(x,t')\,dt'\,dx$, where $t = nT$, with T the period of the applied square wave and n an integer. The solid curve in Fig. 2 is a calculated $\bar{y}(t)$ when μ^n is roughly $6\mu_0$, where μ_0 is the isotropic part of the FLC viscosities. As we see from Fig. 2, the flow velocity $d\bar{y}/dt$ is reduced as time goes on, a result of having less and less FLC drawing on a wider and wider nematic LC area. Alternatively, when there is more nematic in the cell, the pressure gradient $\sigma' \equiv \bar{d}p/dy$ in the FLC grows larger, slowing the flow as shown in Fig. 4 for various cell thicknesses, where the net flow velocities $d\bar{y}/dt$ calculated from $v_y(x,t)$ are plotted as a function of the net pressure gradient σ', for constant square wave field amplitude 8 V/μm. An interesting observation from Fig. 4 is that the net flow velocity decreases almost linearly with increasing

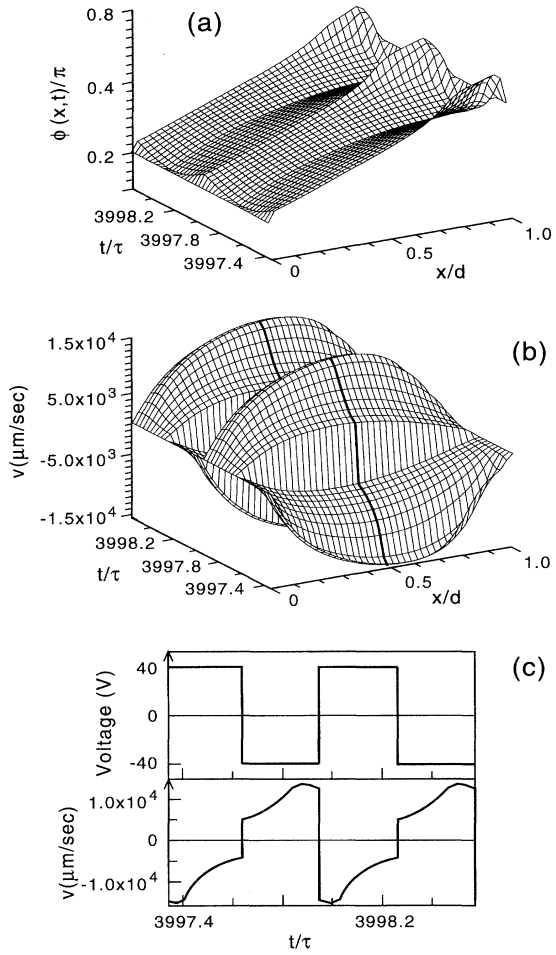

FIG. 3. (a) Typical profile of azimuthal angle $\phi(x,t)$, where d is the cell gap and τ is the FLC characteristic switching time, in this case $\sigma' = 0$. (b) Flow profile corresponding to (a) is due to the nonzero average of $v_y(x,t)$ on x over the cell gap and on t over one period. (c) The applied voltage and corresponding flow velocity at the center of the cell, which is also marked in (b).

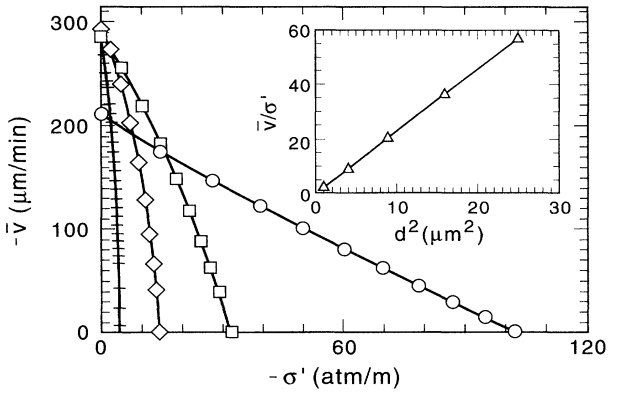

FIG. 4. The calculated net flow velocity $\bar{v}$ vs the net pressure gradient σ'. The calculations have been carried out for different cell thicknesses, with ○, □, ◇, and + for d = 1, 2, 3, 5 μm, respectively. When fitting the $\bar{v}$-σ' curve to the Poiseuille laminar flow equation with back pressure $\bar{v} = (d^2/2\mu_{\text{eff}})\sigma' + \bar{v}_0$, one obtains a linear variation of $\bar{v}/\sigma'$ vs d^2, indicating an effective laminar flow viscosity that is independent of $\bar{v}$ or σ'. $\bar{v}/\sigma'$ of the inset is in $(\mu\text{m/min})/(\text{atm/m})$.

σ'. This linear decrease is simply a result of the Poiseuille laminar flow response to the increasing back pressures σ'. For the simple case where the pumping mechanism is independent of σ', one has $\bar{v} = (d^2/12\mu_{\text{eff}})\sigma' + \bar{v}_0$. To test this we show in the inset of Fig. 4 the slopes $\bar{v}/\sigma'$ of linear fits to the $\bar{v}$-σ' curves in Fig. 4, plotted as a function of d^2. The resulting slope gives $\mu_{\text{eff}} = 2.2$ P, which is comparable to the isotropic component of the viscosity $\mu_0 = 1.875$ P. This behavior indicates that the system is in the regime where the increasing back pressure does not alter the flow-orientation coupling significantly, generating a laminar-flow-like σ' dependence. These results show that significant pressure can be generated in closed ($\bar{v} = 0$) cells.

In conclusion, we have provided direct experimental evidence for pumping by molecular reorientation in LC's. The flow velocity in the pumping effect depends on the cell gap, the surface treatment, and the molecular orientation profile of the cell, and the shape, amplitude, and frequency of the applied voltage. The LSN theory is in good qualitative agreement with the experiment.

The authors acknowledge many useful discussions with Dr. Y. Inaba and other researchers at Canon. This work was supported in part by ARO Contract No. DAAH04-93-G-0164, NSF Engineering Research Optoelectronic Computing Systems Center Grant No. CDR 9015128, NSF DMR Grant No. 9224168, and Colorado Advance Technology Institute.

[1] See a review by F. M. Leslie, Adv. Liq. Cryst. **4**, 1 (1979), edited by Glenn H. Brown.
[2] C. J. van Doorn, J. Appl. Phys. **46**, 3738 (1975).
[3] D. W. Berremann, J. Appl. Phys. **46**, 3746 (1975).
[4] Z. Zou, N. A. Clark, and T. Carlsson, Phys. Rev. E **49**, 3021 (1994).
[5] F. Brochard, P. Pieranski, and E. Guyon, Phys. Rev. Lett. **28**, 1681 (1972); P. Pieranski, F. Brochard, and E. Guyon, J. Phys. (Paris) **34**, 34 (1973).
[6] Z. Zou, N. A. Clark, and T. Carlsson, Jpn. J. Appl. Phys. **34**, 560 (1995).
[7] T. Carlsson, F. M. Leslie, and N. A. Clark, Phys. Rev. E (to be published).
[8] F. M. Leslie, I. W. Stewart, and M. Nakagawa, Mol. Cryst. Liq. Cryst. **198**, 443 (1991).
[9] A. Jakli and A. Saupe, Liq. Cryst. **9**, 519 (1991); Mol. Cryst. Liq. Cryst. **263**, 103 (1995).
[10] This method was suggested by the Canon FLC group in a private communication.
[11] Z. Zou and N. A. Clark (unpublished).
[12] N. A. Clark, T. P. Rieker, and J. E. Maclennan, Ferroelectrics **85**, 467 (1988).

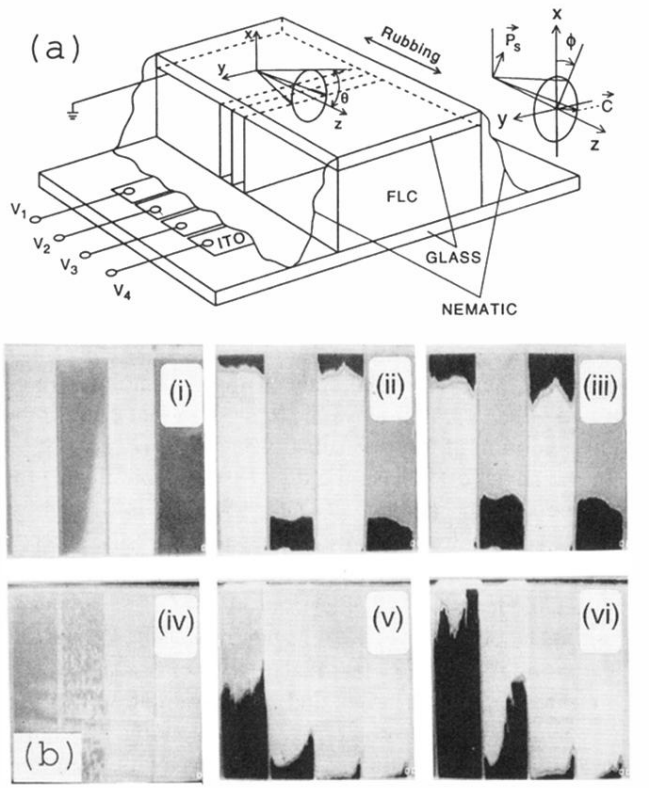

FIG. 1. (a) The SSFLC cell used in the pumping experiment. The cell is unsealed where the smectic layers intersect the cell edge. A second fluid, in this case a nematic, covers the unsealed edges so that if the FLC exits the cell the resulting void can be filled with minimal energy interfacial energy. The ITO electrode in the bottom plate is divided into four pixels. (b) Photo images of SSFLC cells under crossed polarizers show unidirectional pumping. The black areas are the nematic LC drawn into the cell. Photos (i)–(iii) are for a $d = 5$ μm cell with a 10 kHz, 80 V peak-to-peak square wave applied voltage, applied for $t = 0$, 10, and 24 min, respectively. Pixels $(2,4)$ and $(1,3)$ are held in opposite polarization states by a ± 1.7 V dc bias, respectively. Flow goes in one direction for the $(\vec{P}_s)_x > 0$ (white) state, and in the other direction for the $(\vec{P}_s)_x < 0$ (dark) state. Photos (iv)–(vi) (at $t = 0$, 11, and 21 min, respectively) show the voltage dependence of pumping for a $d = 10$ μm cell, pixels 1 to 4 are having 160, 120, 80, and 40 V peak-to-peak square wave voltage applied, respectively. The dc offset is -2 V. The pumping is faster as the voltage increases.